*Annu. Rev. Earth Planet. Sci. 1991. 19:237–62*


# FRACTALS IN ROCK PHYSICS

*A. H. Thompson*

Long Range Research Division, Exxon Production Research Company, P.O. Box 2189, Houston, Texas 77252-2189

KEY WORDS: rock permeability, mercury injection, percolation theory, petrography, porous media

## INTRODUCTION

The concept of fractals, introduced by Mandelbrot (1982), has proven to be a highly useful way to describe the statistics of naturally occurring geometries. Fluid flow, whether it be the rise and fall of rivers (Bridge & Jarvis 1982), turbulence in air or water (Nelkin 1989), or precipitation (Mandelbrot & Wallis 1968), is found to follow self-similar patterns in time and space. Natural objects, from mountains and coastlines (Mandelbrot 1982) to the perimeters of forests (Loehle 1983), are found to have boundaries best described as self-similar, appearing the same on all length scales and having a measured size that depends on the scale of the measurement. Microscopic processes of diffusion (Orbach 1989) and chemical reaction kinetics (Kopelman 1988) can lead to fractal structures, while the scale independence of natural processes can lead to the ubiquitous $1/f$ noise and stretched exponential relaxation (West & Shlesinger 1990). Many review articles and books have been written on fractals [see Hurd (1988) for a bibliography], and reviews (Wong 1988) and conference proceedings (Scholz & Mandelbrot 1989, Aharony & Feder 1989, Fleischmann et al 1989, Avnir 1989) have appeared on various aspects of fractal applications in geophysics.

I do not attempt to review here basic fractal concepts as they are covered in the cited literature but rather concentrate on fractal structure at the microscopic scale in sedimentary porous rock and on the geometry of flowing fluids. One objective of this work is to develop models for rock pore geometry that will distinguish rocks from other porous materials. The length scales of interest include the submicron structure on pore walls,



0084–6597/91/0515–0237$02.00

the hundreds of microns structure in pore volumes, and length scales up to the order of centimeters, where a collection of grains can first be described as having the properties of a bulk rock. These geometrical studies are the first step in establishing scaling relations between properties measured at the laboratory and field scales.

A second objective of this work is to identify connections between the geometry of flowing fluids in rock pores and the transport properties, such as flow permeability. The pore geometry of many sedimentary rocks is determined by the processes of crystal dissolution and growth that are themselves closely related to fluid flow. Even though there is no known general analytical relationship between the complex geometry of a pore space and the transport properties of fluids in that pore space, we would like to know if sedimentary rocks are a special case where geometry and transport are closely connected. If they are connected, then ties between various physical properties may be established that could permit improved remote measurements of permeability and direct hydrocarbon detection. General rules connecting geometry and transport in rocks could be possible if the pores of interesting rocks can be described by a small set of geometrical statistics, such as fractal statistics.

## FRACTAL CONCEPTS FOR POROUS ROCK

The fractal properties of interest to rock physics can be described by qualitative concepts. Figure 1 is a scanning electron photomicrograph of a fracture surface of a sandstone taken from Thompson et al (1987a), where its fractal properties were discussed. Qualitatively (statistically), the structure seen in Figure 1 appears similar as the magnification is increased. This structure is described as a stochastic fractal if there is a power-law relation between the number of grains or surface irregularities of size $l$ and the size $l$. Measurements of the fractal properties must determine both the distribution of pore or surface sizes and the correlation between sizes. If the grains of size $l$ were all clustered together, then there could be long-range order not characteristic of fractals. In each case the fractal character resides between limits $l_1$ and $l_2$ that define the lower and upper scale boundaries of the structure, respectively. The lengths $l_1$ and $l_2$ and the fractal dimension (the exponent in the power-law size distribution) are the statistics needed to define a pore fractal.

The fractal structure of Figure 1 might be described as a fractal quilt, a patchwork fractal, or a multifractal. Regions smaller than some size $l_2$, typically a size close to the largest grain size, have surface and/or volume fractal character. Different locations in a rock of size less than $l_2$ may have slightly different fractal dimensions and fit together at graded or fractal-

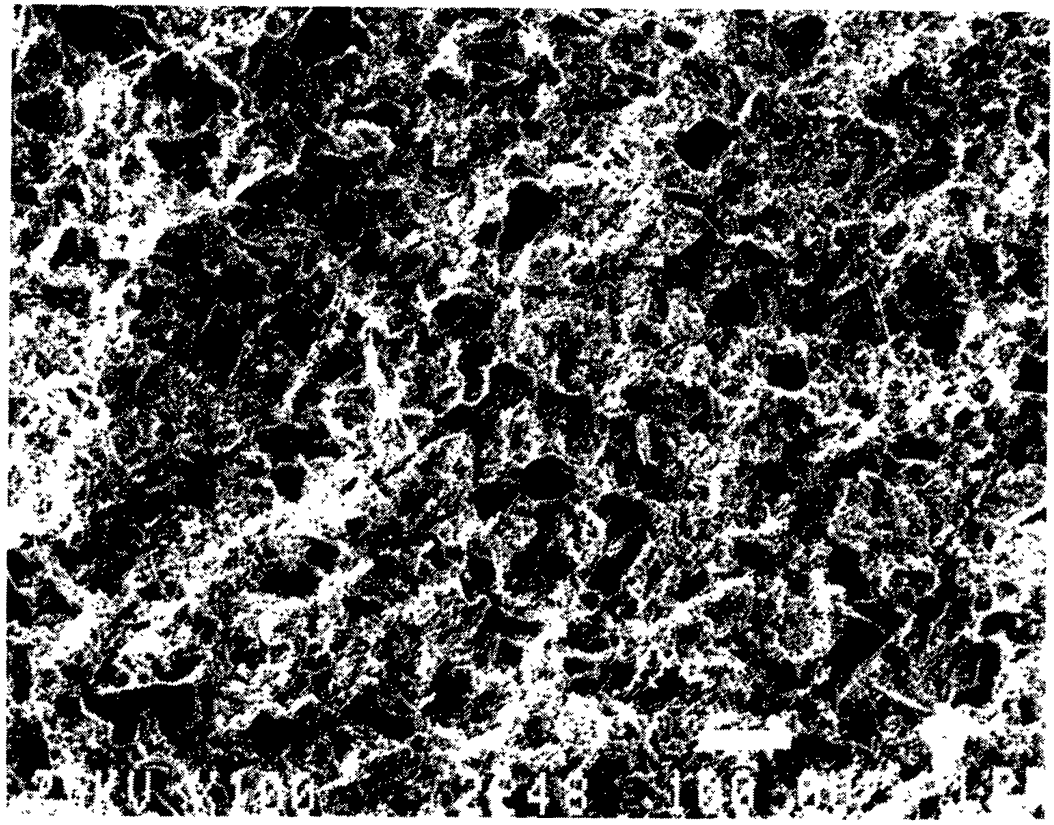

*Figure 1* Scanning electron photomicrograph of a highly diagenetically altered sandstone.

defect boundaries. The $l_2$ values may have a Gaussian distribution and vary from one location in the rock to another. Measurements on the whole quilt then yield average values of $l_2$ and the fractal dimension $D_F$. The details of such a model recently have been discussed by Nigmatullin (1989).

The structure on a fracture surface such as shown in Figure 1 contains a small number of defects introduced by rock fracture. These defects, such as grains plucked from the surface, comprise perhaps 10% of the observed surface for a typical sandstone, whereas the remainder of the surface structure is characteristic of the pore structure.

The rock pore geometry conveniently can be divided into the surface geometry, the single-pore-volume geometry, and the collective geometry of all of the pore space. The surface geometry of interest may extend from atomic dimensions of a few angstroms up to the size of the pore volume (hundreds of microns) if the pore surface is so complex as to be space filling. The pore volume geometry may be thought of as two-dimensional ribbons, or as tubes or spheres in cases where the pore wall is relatively smooth. In other cases, the roughness of the pore wall is so great that separating the pore wall from the pore volume is not meaningful. The

ensemble of pores is often modeled as a collection of tubes on a lattice or as the interstitial region in a glass-bead pack. Such simple packings lead to notions of pore throat and pore bodies, but in sedimentary rock the definition of throats and bodies is questionable, and the dissolution and precipitation associated with pore-fluid flow leads to pore-to-pore correlations that may not be described well by random flow models. An all-encompassing geometry of rock pores will probably require a multifractal description in which the concepts of surface, volume, throat, body, etc, are blurred by the evolution of the geometry from one scale to another. However, the present discussion treats the pore surface, volume, and ensemble of pores as separable concepts as a means of summarizing the present literature.

## FRACTAL MEASUREMENTS ON SEDIMENTARY ROCK

### *Discrete Methods*

The discrete methods for fractal measurements are based on the earliest descriptions of curves with nonintegral dimensions (Mandelbrot 1982, and references therein). In these methods the size or measure of the fractal object is determined by using rulers of different lengths. Perhaps the best known example is the measurement of the length of the coastline of an island using dividers of different sizes. A fractal coastline will have a length that increases in power-law fashion as the divider size decreases. Alternatively, the coastline could be covered with circles of one size and the number of circles required determined as a function of circle size. These discrete, direct methods are robust and convincing ways to measure $D_F$. In practice, such methods are often difficult to implement because the geometry in question must be digitized with high spatial resolution so that precise power-law relations can be observed over more than one decade in length scale.

In one of the earliest direct measurements of $D_F$, Kay (1986, and references therein) characterized the shape of fine particles of carbon black using a two-dimensional projection and estimated the fractal dimension to be 1.32 from data covering one-half an order of magnitude in length scale. In similar work, Orford & Whalley (1983) attempted to discriminate between various sedimentary particles based on their fractal character. Fractal dimensions between 1.0 and 1.3 were reported. Different particle types were distinguished on the basis of both the fractal dimension and the length scales over which fractal behavior was observed. The limited set of length scales available to these studies, the closeness of $D_F$ to 1.0,

and the limited statistics available from data on single particles lead to uncertainties in the fractal interpretation of particle structure. Farin et al (1985) have highlighted problems with a fractal analysis on these small data sets. Clark (1986) has described several approximate divider methods for a more rapid determination of an approximate $D_F$ on particle shapes, but these methods are also limited by the small data sets available on single particles.

Ensembles of particles in sedimentary rocks provide opportunities to develop good statistical relations over many orders of magnitude in length scale. Hansen & Skjeltorp (1988) cover the pore volume and pore surface observed on thin sections with boxes of various sizes. Surface and volume fractal dimensions of 2.59 and 2.73 were determined for a North Sea sandstone. These box-counting methods are selective to pore volume and pore surface fractals, and good statistics can be accumulated by choosing many different locations for the centers of boxes. They are limited in that they can be readily applied only to thin sections where edges (pore surfaces) and volumes can be distinguished. Also, thin-section resolution is typically limited by the polishing process to 1 $\mu$m. The Hansen & Skjeltorp results do not permit a direct calculation of either the fractal pore volume or the surface pore volume for comparison with measured porosity because the limits of the fractal region are not reported. A comparison of the fractal volume with measured porosity would lend support to the physical relevance of the fractal measure. Such a comparison for the North Sea sandstone is particularly important because the fractal regime extends beyond the size of the largest grains, and because the log-log plot for the surface structure is nonlinear, indicating departures from fractal scaling.

The fractal dimension of the pore-grain interface may also be inferred by measuring the chord-length distribution formed by intersections between a line and the pore surface (Thompson et al 1987a). The principle of these measurements is shown in Figure 2 for a thin section and a fracture surface. Both measurements determine the same parameter—the distribution of chord lengths terminated by the interface. Note that chord length is measured in both rock and pore regions. For a fractal interface, the number of chords of length $l$ will form a power-law relation with the chord length $l$, and the power-law exponent gives the fractal dimension. No correlation information is contained in the chord-length distribution, so a power-law correlation establishes a necessary but not sufficient condition for fractal structure. This disadvantage is balanced against the advantage that the chord-length measurements can be done on both thin sections and fracture surfaces, using both optical and electron microscopes, and so cover length scales ranging from 1 cm to $10^{-5}$ cm (0.1 $\mu$m). Chord-

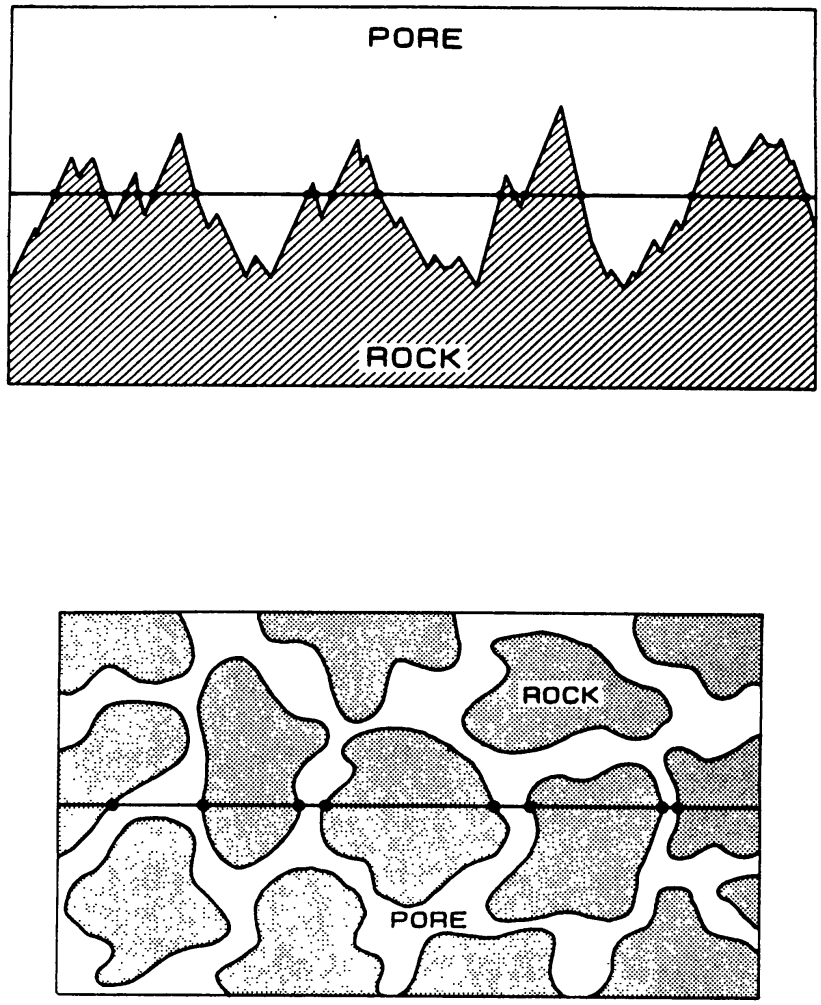


*Figure 2* Schematic illustrations of chord-length measures of the fractal dimension of a pore-rock interface. The *top frame* illustrates measurements on a fracture surface, while the *bottom frame* represents a thin section.

length distributions are also sensitive to the length-scale limits for fractal behavior and do not mix interpore and intrapore correlation information.

Chord-length measurements for two sandstones are shown in Figure 3. The top part of Figure 3 shows a case where the fractal structure continues over the whole range of measurement, while the bottom part shows a crossover to homogeneous, nonfractal behavior near 10 $\mu$m. The data of Figure 3 are plotted such that the slope is $3-D_F$, so that a homogeneous region has zero slope. This manner of plotting the data sensitively reveals deviations from power-law behavior. Log-log plots made with a slope of $D_F$ tend to hide systematic errors in the data and should not be trusted to support conclusions about fractal structure.

A direct measurement of the size distribution of pore volumes on a thin

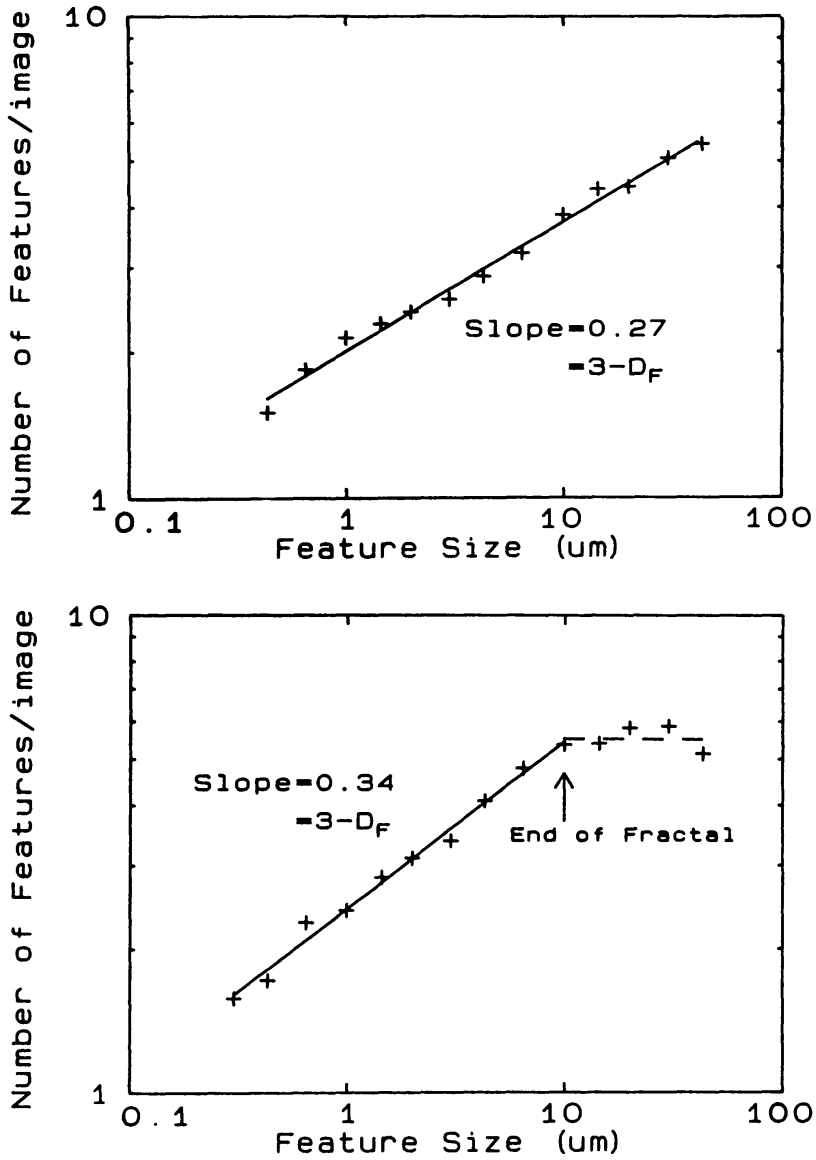


*Figure 3* The results of chord-length measurements on two sandstones. The *top frame* is for the sandstone of Figure 1, where the upper end of the fractal region is not detected. The *lower frame* is for a second sandstone, where the crossover to the homogeneous region is near 10 $\mu$m (Krohn & Thompson 1986).

section can be used to estimate the nonfractal portion of the pore volume and the distribution of pore volumes above the fractal-to-Euclidean crossover (Krohn 1988a). The pore volume distribution is determined by counting the number of volume elements of length $l$ having cross-sectional area of one pixel. This number of volume elements is then plotted versus the length $l$. Figure 4 is a plot of the pore-volume distribution and the cumulative porosity for the sample of Figure 1. Below 6 $\mu$m the power-law

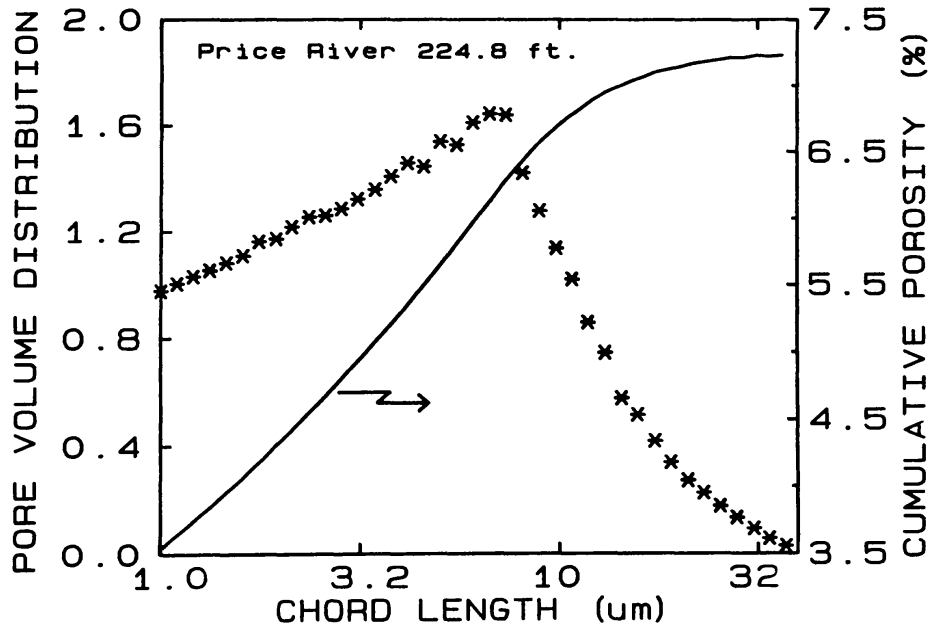


*Figure 4* The pore-volume distribution (*points*) and the cumulative porosity (*solid line*) measured on a thin section for the sample of Figure 1. The sample is from the Price River formation in Utah. The cumulative porosity shows that most of the pore volume lies at length scales in the fractal, power-law region below 6 $\mu$m (Krohn 1988a).

distribution of volume elements is in the fractal regime, whereas above 6 $\mu$m the pore-volume distribution is exponentially decaying. The data of Figure 4 show that for that rock the fractal volume accounts for most of the pore volume. The fractal porosity can be estimated from the relation $\phi = (l_1/l_2)^{3-D_F}$, where $l_1$ and $l_2$ are the lower and upper limits of the fractal region, $D_F$ is the fractal dimension, and $\phi$ is the porosity (Katz & Thompson 1985). This relation for porosity was used to calculate $\phi$ for a group of sandstones whose pore space is dominated by fractal structure. The length $l_2$ is experimentally determined, while $l_1$ is an adjustable parameter assumed to be the same for all the samples. The measured and calculated porosities were found to be in good agreement with $l_1 = 2$ nm (Thompson et al 1987a). The 2-nm, molecular length scale is consistent with generation of fractal structure on pore surfaces by crystal growth and nucleation (Katz & Thompson 1985) and is consistent with an empirical connection between fractal structure and clay content (Wong et al 1986). The agreement between calculated and measured porosities lends support to the conclusion that the fractal parameters measured on those samples are measures of pore volume.

The exponential decay of volume elements at $l_2$, as shown in Figure 4 above 6 $\mu$m, may be typical of the boundaries of fractal regimes in natural

systems. The power-law region would be expected to end smoothly because the fractal-quilt picture suggests that there is a distribution of fractal dimensions and $l_2$ values. The exponential decay may indicate a Gaussian size distribution of fractal patches.

## *Spectral and Scattering Methods*

The discrete methods microscopically digitize and analyze data in the spatial domain, while the spectral and scattering methods transform to the spatial frequency of wavenumber domain. Among spectral and scattering methods, I consider here small-angle neutron scattering, autocorrelation, and spectral density methods. Generally these techniques have the advantage that the data are either collected as averages over the whole sample with no microscopic digitization or are numerically transformed to the frequency domain where they are analyzed. The disadvantage of these methods is that the interpretation is often model dependent, and the transformed data may not sensitively distinguish subtle differences between two models.

The pore-space autocorrelation function measured on a thin section is closely related to one definition of a fractal pore set (Mandelbrot 1982). If the pore space is fractal, then the probability of finding pore space at distance $r$ falls off as $r^{D-2}$. A measurement of this type on a rock section would, in principle, be an unambiguous test for fractal behavior. In a few cases this measurement is satisfactory for rocks, but in most cases it is not, for two reasons. First, the range of length scales that can be measured is too limited; second, overlapping uncorrelated pores distort the power-law result.

Katz & Thompson (1985) made autocorrelation measurements by a classical optical technique. Backscattered electron micrographs of polished thin sections were photographically enhanced with high-contrast black-and-white film to produce a binary image. Two identical negatives were then made on 35-mm-film format. The two films were placed in an optical microscope to measure the transmitted light through both films. The autocorrelation function is given directly by the transmitted intensity as a function of the distance one film is translated relative to the other.

Figure 5 is a set of results for a fractal pore space that illustrates the information contained in such data. The data are on a log-log plot to identify a power-law component. The $x$-axis is the lag—the translation of one film relative to the other from the position of maximum registry. The $y$-axis is the transmitted intensity and is proportional to the autocorrelation. At small lag the plot is approximately linear but continues over less than one order of magnitude in length scale. At longer lag, the intensity flattens off. This is the behavior expected for a fractal pore space when the

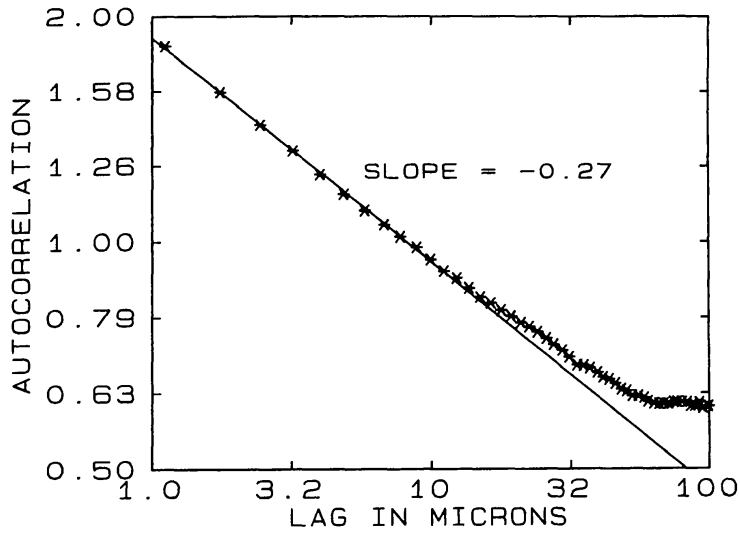


*Figure 5* Autocorrelation measurement of the fractal dimension for the sample of Figure 1. The slope is $D_F - 3$, giving $D_F = 2.73$, in agreement with chord-length measurements (Katz & Thompson 1985).

longer lags introduce overlap between separated pores that are randomly correlated.

Pores that are not connected or that are separated by more than some correlation length $l_2$ are uncorrelated. Power-law behavior is then expected only between the resolution limit of $\sim 1$ $\mu$m and an upper limit set by the appearance of pores that are not correlated with those at zero lag.

The rock sample illustrated by the data of Figure 5 is an excellent example of fractal behavior. This is the same rock sample illustrated in Figure 1, and the $D_F$ value determined from the autocorrelation agrees with that measured by the discrete, chord-length measurement. It is a tight, highly diagenetically altered sandstone from the Mesa Verde formation in Utah. The alteration is so extensive that the sedimentary sand grains are difficult to recognize. Because the pore infilling is so extensive, the whole pore volume is a space-filling fractal, and the fractal structure continues up to the dimension of the sand grains.

In other cases the diagenetic alteration is not so extensive. Only the pore surface is fractal and/or the fractal structure stops short of the size of grains (Krohn & Thompson 1986, Krohn 1988a). In these cases the autocorrelation function has a complex shape with no power-law behavior. The limited length scales available to thin-section measurements and the inhomogeneities and anisotropies encountered in many rocks mediate against the usefulness of autocorrelation measurements for fractal analysis (Thompson et al 1987a).

Power spectrum or spectral density analyses have been made on numerous geologic structures. They have not been widely used for micro-

structural analysis but are included here for completeness. Huang & Turcotte (1989) used the spectral density to analyze fractal maps of land topography on a scale of kilometers; Brown & Scholz (1985) used surface profilimeters to measure rock topography at scales of less than 1 m and analyzed the data using power spectra; Hewett (1986) performed spectral analyses of reservoir heterogeneity; and Wong (1987), Brown (1987), Hough (1989), and Power & Tullis (1988) have discussed the relation between spectral and divider methods. Geologic surfaces may be either self-similar or self-affine fractals. A self-similar surface fractal is like the pore surface fractal, where the processes of crystal nucleation, growth, and dissolution produce three-dimensional structure with overhangs and convoluted shapes. A self-affine surface fractal (Mandelbrot 1986) has different scaling properties parallel and perpendicular to the surface and might be expected to result from anisotropic processes, such as those influenced by gravity (mountain profiles) or by abrasion (some fracture surfaces). A fractal time series would be expected to be self-affine. But as Hough (1989) points out, a power-law relation on a power spectrum is only a necessary and not a sufficient condition for fractal behavior. Nonfractal time series may have power-law Fourier transforms.

Small-angle scattering of X rays or neutrons provides a measure of fractal properties at length scales between 50 and 0.5 nm. Wong (1987) reported the neutron data on a shale and sandstones shown in Figure 6, whereas earlier data by Bale & Schmidt (1984) were taken on coal. The

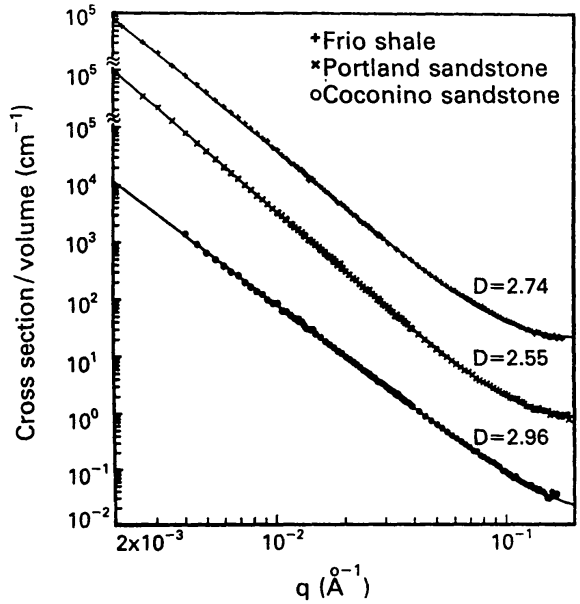


*Figure 6* Neutron scattering data on a shale and sandstones showing fractal surface structure at length scales below a few tens of nanometers. Reproduced with permission from Po-zen Wong (see Wong 1988).

scattered intensity at small angles (small wavenumber $q$) is a power law. For a surface fractal on rock grains the intensity is $I(q) \propto q^{-(6-D_F)}$, while for a volume fractal the intensity is $I(q) \propto q^{-D_F}$ (Bale & Schmidt 1984). The scattered-intensity power law then has an exponent lying between 3 and 4 for a surface fractal, and between 2 and 3 for a volume fractal. The data of Figure 6 show that below a few tens of nanometers the scattering is sensing surface fractal structure. Limestones and dolomites were found to have smooth surfaces at these length scales. Lucido et al (1988) find a similar surface fractal result for certain volcanic rocks, but in several examples the power-law exponent is so close to $-4$ that fractal surface scattering is not distinguishable from scattering from smooth particles (Porod scattering with $d = 2$).

These small-angle scattering studies establish that the scattering at molecular length scales is dominated by a surface fractal on the pore wall. The results do not provide evidence concerning pore-volume fractals at other length scales. Although the small-angle scattering found smooth surfaces in limestones and dolomites, Krohn (1988b) found fractal pore volumes in carbonates at length scales greater than 100 nm using image analysis of electron photomicrographs. In some cases, such as the example of bedford limestone, the individual grains are smooth, but the broad distribution of grain sizes and their packing arrangement lead to a fractal pore volume. The issue of having a fractal pore volume over many orders of magnitude in length scale has led to some controversy (Roberts 1986, Katz & Thompson 1986a). If the pore volume were a perfectly self-similar fractal over a length-scale interval of, say, 2 nm to 100 $\mu$m, then it could be argued that the largest free volumes would be of the order of 2 nm. Also, it is known that for some model self-similar structures, a surface fractal bounding a volume fractal will not have the same fractal dimension (Hansen & Skjeltorp 1988), and indeed the volume enclosed by a surface fractal need not be fractal. These concerns, based on ideally self-similar fractals, are not relevant to real world, stochastic fractals, where we expect to see Euclidean defects terminating the fractal region at both the large and small length limits of the fractal region (Figure 4), and where we can expect to see both surface and volume multifractals. Sinha (1989) has discussed the general case of scattering from mass and surface fractals with length-scale cutoffs $l_1$ and $l_2$.

In recent X-ray and neutron scattering studies (Hurd et al 1989), the small-angle scattering calculation of surface area was compared with surface area measured by adsorbates. High-surface-area silica and carbon samples were studied. The samples had fractally rough surfaces that behaved as if the surface area increased as the fractal dimension approached 3. The data support the surface fractal models for scattered

intensity and calibrate the surface adsorption methods used to measure fractal dimension.

Small-angle scattering from fractal porous media has been of interest in model systems related to applications such as catalysis. Rojanski et al (1986) report multiple surface measurements on silica gel. Freltoft et al (1986) discuss the effects of finite cluster size on scattering measurements. Sharp cutoff lengths $l_1$ and $l_2$ result in slow changes in slope of the scattered intensity curves and complicate the interpretation in those cases. Sinha et al (1988) calculate the scattered intensity from rough surfaces, including self-affine fractals. A review of the literature on small-angle scattering is beyond the scope of this article; the reader is instead referred to this cited literature.

## *Adsorption Methods*

In addition to small-angle scattering, the fractal structure of surfaces at molecular length scales can also be investigated by molecular adsorption. In one of the earliest experiments on fractal surfaces, Pfeifer & Avnir (1983) and Avnir et al (1983) reported data on surface coverage as a function of molecule size. The idea is that molecules of various sizes can be used as molecular-scale yardsticks to measure the area of a fractal surface as a function of the size of the yardstick. The number of molecules required to form a monolayer was measured for different molecules and for one molecule on samples with different surface areas. Fractal dimensions between 2 and 3 were obtained on a variety of powdered samples. Avnir et al (1984) tabulated similar measurements on numerous materials, including igneous and sedimentary rock. Pfeifer (1987) has reviewed the adsorption methods in context with other measurement means. In addition to quantitatively measuring the adsorbed gas at one monolayer, adsorption isotherms (Pfeifer et al 1989, Albano & Martin 1989) and molecular dynamics (Drake & Klafter 1990) can be used to determine surface or pore properties at molecular dimensions. Drake & Klafter (1990) find that the molecular dynamics of fluids in porous silica glasses can be characterized by an effective average pore size, and a fractal pore geometry is not needed to explain the data.

Adsorption methods may, in some circumstances, yield biased values of the fractal dimension if chemical disorder on surfaces is a dominant factor, or if molecular orientation or conformation is a function of coverage or surface structure. These problems have been addressed by systematic studies with molecules of various sizes and internal structures (Meyer et al 1986). It further was suggested (Fripiat et al 1986) that molecular adsorption does not ideally cover the interface (the molecule would have to penetrate the solid to do this) but instead resides on the surface on one

side of the interface. On extremely complex surfaces with $D_F \sim 3$, portions of the surface may shadow neighboring surface, leading to incomplete adsorption and an underestimate of $D_F$. There is also a potential ambiguity as to when a monolayer coverage is achieved (Hall 1986). However, these concerns have not proven to be of general significance in studies on geologic materials, where measured values of $D_F$ are in approximate agreement with those obtained by other means.

## *Summary of Methods*

Numerous methods have been used successfully to determine the microscopic fractal properties of porous rock, each having its own utility. The choice of method depends on the questions being asked and the length scales of relevance. Almost all sedimentary rocks have some region of fractal structure, and the existence of robust power-law distributions is not an issue. [The only counterexample known to the author is novaculite, a metamorphic, porous rock with no apparent fractal structure (Thompson et al 1987a).] Sandstones and shales generally have fractal pore surfaces at molecular dimensions below 500 Å. These fractal surfaces may evolve into fractal pore volumes at pore sizes, in which case the total porosity can be estimated from a calculation of the fractal measure. Our experience suggests that ~15% of measured samples fall in this category. In the remaining cases there are varying degrees of pore-filling fractals. Carbonates may be formed by different processes from those involved in sandstone diagenesis and hence have different structures. The molecular-scale surfaces may or may not be fractal, while the pore volume may be fractal even when the individual grains are smooth, just as if such a rock were constructed from a distribution of spheres or cubes in the same manner as numerically generated fractals.

All of the fractals discussed here are at the pore scale or below. In general, interpore fractal correlations have not been reported, but such studies have not been exhaustive. The molecular-scale fractals are of interest in understanding gas adsorption measurements of surface area, rock wettability, diagenesis, and petrography. The larger scale structure is of interest in its impact on rock transport properties, particularly the electrical conductivity in shaly rock (Sen 1989, Schwartz et al 1989) and flow permeability (Thompson et al 1987a).

The length-scale limits of the fractal regions may help to define the scales where physical properties should be governed by one set of processes. In this regard it would be interesting to know the upper boundary for the surface fractals seen at molecular dimensions so as to better quantify the surface influence on transport properties and surface conduction in particular.

# FRACTALS AND TRANSPORT PROPERTIES

Fractals enter the problem of fluid transport in porous media in at least two distinct ways. First, the fractal pore-structure information might be used directly to calculate the conductivity and permeability of porous rock. Second, the paths formed by flowing fluids or ions in pores may be described by fractal models such as result from percolation theory. In this second alternative, the pore space may be the model fractal, or the path generated by the flowing fluid could be the percolation cluster independent of the underlying pore geometry. Here I briefly summarize work of the first kind—calculating transport on fractal or random structures—but spend more time on the percolation problem as it is applied to rock materials.

## *Models Connecting Pore Geometry and Transport Properties*

Adler and coworkers (Adler 1989) have pioneered the development of permeability models on well-defined, deterministic fractal structures. Stokes equations are solved for one- to three-dimensional geometries of single or multifractal character. The systematics developed may help establish ties between the geometric concept of the fractal dimension of the pores and the transport properties like permeability. Such connections between geometry and transport might be generalized to more complicated or statistical fractal structures. Recent work (Adler 1989) is aimed at generating networks having the statistics of rock-pore systems. One interesting result from these calculations is that one-dimensional fractal lattices produce results consistent with the classical Kozeny-Carman relation for permeability [$k \sim \phi m^2/c$, where $\phi$ is the porosity, $m$ is the hydraulic radius (or the pore volume divided by the wetted surface area), and $c$ is a constant. Numerous variations of this relation exist in the literature (Dullien 1979)]. The Kozeny-Carman relation is based on a tube model that weights all pore surface and pore volume equally and would be expected to work best in situations such as the one-dimensional example, where all pores are constrained to carry flow.

Berryman & Blair (1987) use an approximate image analysis approach to define the pore-size parameter (the hydraulic radius) in the Kozeny-Carman relation. Since (*a*) only the larger pores are expected to dominate the flow properties and (*b*) microscopic surface roughness will have a minimal effect, the pore space is assumed to be Euclidean, and a low-magnification image is used to generate an effective volume-to-surface ratio. This method will directionally give an improved connection between geometry and transport but does not account for correlation in the pore

space among pores of different sizes. Although there are the several assumptions and approximations invoked in this method as noted, Berryman & Blair get reasonable correlations with measured permeability.

In another approach to connecting geometry to permeability, the permeability is rigorously calculated for a periodic array of spheres at low sphere density (Zick & Homsy 1982). This exact result is one bound on permeability at low sphere density. Disorder on the sphere lattice renders the problem intractable, but upper bounds on the permeability can be derived using variational methods (Weissberg & Prager 1970). In general, the permeability of a random porous medium depends on an infinite set of geometrical parameters—for example, an infinite set of correlation functions. This set of statistics will not be known for natural media like rocks. Weissberg & Prager (1970) showed that upper bounds can be obtained using only correlation up to three-point correlation functions. Berryman & Milton (1985, 1988) have extended the bounds to include joint bounds on the electrical and thermal conductivities, the shear and bulk modulus, and the electrical resistivity formation factor. Torquato & Beasley (1987) extended the bounds to include overlapping spheres and suggest that for large overlap the Kozeny-Carman relation will be close to the computed upper bound. Rubinstein & Torquato (1989) further bracket the permeability by establishing a means for computing a lower bound on permeability. Torquato & Lu (1990) and Torquato (1990) consider the case of a distribution of sphere sizes and draw an interesting tie between the traps that regulate diffusion-limited reactions and the permeability. This last point could help tie rock diagenesis to permeability.

The permeability bounds discussed above use the statistics of the $n$-point correlation functions that define pore geometry to derive transport properties. Fractal statistics may also be used to define the pore geometry. The fractal dimension is the first statistic in an infinite series of statistics. The second higher order, geometrical statistic might be the correlation between regions having the same fractal dimension (Thompson et al 1987a). Stanley (1984) has discussed the fractal statistics needed to specify various physical properties. These statistics are geometrical but may not be measurable using micrographs. For example, the fractal described by the subset of pores making up the connected path of largest pores is not apparent on a micrograph but might be available by injecting a sample with liquid metal and measuring the geometric properties of the metal path when the first connected path is formed. Similarly, other fractal statistics that measure how far a particle diffuses before it reacts with the wall, or the fractal dimension of a growing cluster of crystals, may be of central importance in describing some physical process but, in general, are not easily measured.

## *Effective Pore Size Models*

The flow permeability of a porous medium has units of length squared; it is proportional to the cross-sectional area of some effective pipe size. The problem of estimating the permeability from other physical or geometric measurements may be reduced to posing the question, "What is the effective pore size for permeability?" Historically, this question was answered by assuming that the *only* characteristic length in a rock pore space is the volume-to-surface ratio $V/S$ (Scheidegger 1960, Dullien 1979). This assumption led to the Kozeny-Carman relation $k = (V/S)^2(\phi/C)$, as discussed in the previous section. Although this expression works very well for some simple geometries, its accuracy will be poor (*a*) when there are many small, high-surface-area pores; (*b*) when there are rough large pores with surface structure that does not contribute to flow; and (*c*) when there are large pore volumes accessible only through small pores that increase $\phi$ without increasing permeability. The effective pore size is obviously a function of all the geometrical parameters needed to estimate permeability from geometry, i.e. an unbounded set of statistics. It is not generally available from a single, strictly geometric measure, no matter how cleverly that length might be chosen. Alternatively, the length parameter entering the permeability can be viewed from the start as a transport property, and a transport measurement other than permeability might be designed to measure that length. I next describe two approaches to transport measurements of the permeability length scale.

THE MERCURY INJECTION LENGTH SCALE This approach to estimating permeability starts with the assumption that the pore space can be represented by a network of tubes. The tubes may be smooth pipes or fractally rough pores. The tubes on the network have a broad distribution of sizes, and they are randomly placed on the lattice. [The condition that the distribution of sizes is broad is not a severe requirement because when the pore diameter and length are the same, the hydraulic conductivity is proportional to the cube of the pore radius. A factor of 2 or 3 in pore radius will lead to a factor of 10 in the width of the hydraulic-conductance distribution (Katz & Thompson 1986b).] There are no long-range correlations (on the order of the sample size) in the size of tubes. When a rock sample can be assumed to fit this model network, the transport properties on that network and for that rock can be treated as a percolation problem.

Percolation theory has proven to be a very powerful technique for modeling transport processes in random materials (Stauffer 1985). Ambegaokar et al (1971), Shante (1977), and Kirkpatrick (1979) have argued in the context of amorphous semiconductors that transport on a disordered lattice can be approximated by assuming that electrical con-

ductivity is dominated by transport through a subset of the most highly conducting bonds. Katz & Thompson (1986b) have extended these ideas to flow in porous media, where they suggest that permeability will be dominated by flow on an effective path of large pores defined by mercury injection. The most effective transport path can be visualized by progressively filling the pores one at a time, starting with the largest pore. At some critical point, filling one additional pore will create a connected path across the sample and fluid will flow. As additional pores are filled, the capacity of the lattice to carry fluid will increase because the number of pores and paths is increasing, but each additional pore is less and less effective because it is smaller in diameter. Since the hydraulic conductance of each tube decreases faster than the filled volume increases, the smallest pores make a vanishingly small contribution to the total permeability. The path that is created when the first connected cluster is formed is called a percolation cluster. In three dimensions it is a fractal with a fractal dimension of 2.5 (Alexander & Orbach 1982). Note that in this model the pore space has fixed geometry and the fluid is filling that geometry. The fluid is percolating onto the lattice. The pore lattice is not a variable being constructed in this process.

Katz & Thompson (1986b) recognized that mercury injection defines the first connected path and, hence, the diameter of the smallest pores on that path (see also Charlaix et al 1986, Baudet et al 1987, Gueguen & Dienes 1989). This smallest pore size on the connected path of largest pores will be the required length $l_c$ defining the permeability pore size. When mercury, a highly nonwetting fluid, is injected into a porous rock, it seeks to occupy the largest pores at each capillary pressure. The electrical conductivity across a sample can be measured to determine the point where a connected path is formed. The pressure at that point can be related to the effective pore size by the Washburn equation, $l = 4\gamma \cos \phi / P$, where $l$ is the pore diameter, $\gamma$ is the surface tension, $\phi$ is the contact angle, and $P$ is the pressure. The absolute permeability is related to the mercury injection by the relation (Katz & Thompson 1986b),

$$k = \frac{1}{226} l_c^2 \frac{\sigma}{\sigma_0}, \tag{1}$$

where $l_c$ is the threshold length from mercury injection empirically determined to be at the inflection point on a mercury-injection curve [recent numerical simulations also find electrical continuity at the inflection point (E. J. Garboczi & D. P. Bentz, submitted for publication)], $\sigma$ is the rock electrical conductivity, and $\sigma_0$ is the conductivity of the fluid filling the pore space. The constant 226 is not an adjustable parameter but rather is

a result of the percolation model calculations. It arises from the fact that not all of the flow can be assumed to occur right at the threshold condition, and the dominant paths for conduction and fluid flow are not the same. The approximations in the model indicate that the constant should be accurate to within approximately a factor of two. Banavar & Johnson (1987) and Doussal (1989) calculate slightly different values using other approximations.

Equation (1) is very simple and superficially similar to a tube-model expression for the permeability, but it has much broader applicability than do tube models. It is expected to correctly estimate the permeability to within a factor of two for all rocks, satisfying the general model assumptions. Figure 7 is a plot of measured absolute permeabilities vs those estimated from mercury injection using Equation (1). We find that the agreement is generally within a factor of two except for cases where there are clear experimental problems associated with either measurement errors at low permeability values, sample inhomogeneities, or cracked samples. We do not find any systematic deviations, as suggested by Kamath (1988), in the permeability/mercury-injection correlation. (When comparing measured and calculated absolute permeabilities, care needs to be taken to use only permeabilities measured by gas flow extrapolated to infinite pressure.) A least-squares fit to the data yields a slope of 0.997 and a constant of 197 instead of the ideal value of 226, well within the expected model uncertainty of a factor of two. We have had excellent success in applying the mercury-injection estimate of permeability to sandstones, carbonates, and meta-

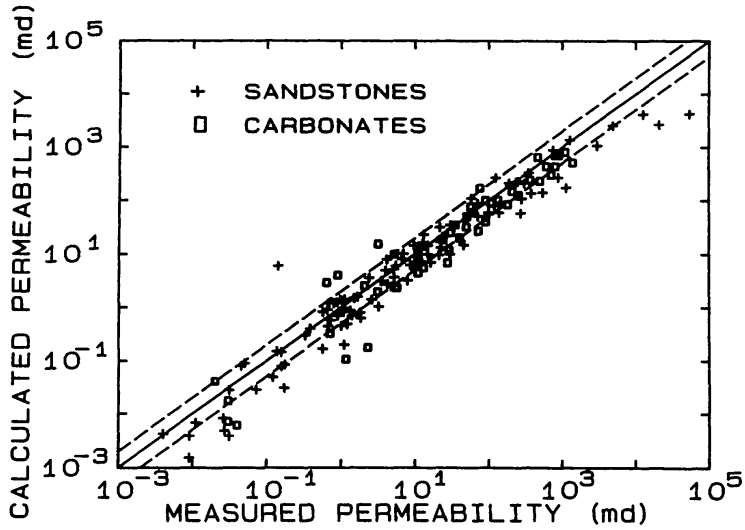


*Figure 7* Comparison between absolute permeability measured by gas flow and that calculated from mercury injection using Equation (1). The *solid line* is in agreement with Equation (1), while the *dashed lines* display a factor-of-two variation.

morphic rocks on samples ranging from 1 $mm^3$ to 10 $cm^3$. The data of Figure 7 are representative of measurements made on several hundred samples.

Well before the percolation description of mercury injection and permeability, there were empirical correlations established between mercury-injection curves and permeability. The earliest attempts reasoned that the complete injection curve was needed to define permeability (Dullien 1979). In rock studies, Swanson (1981) first noted that the effective path could be identified from mercury injection but chose parameters that yield the effective path for conductivity instead of permeability (Thompson et al 1987a). Nyame & Illston (1980) found an empirical parameter similar to $l_c$ to describe permeability in cement paste, whereas Lukasiewicz & Reed (1988) applied a mean-entry, pore-radius analysis to porous alumina.

LOCAL ELECTRIC FIELD PORE SIZE Johnson et al (1986) proposed a new pore-size parameter, $\Lambda$, that is the pore volume-to-surface ratio weighted by the electric field across the pore. This parameter is a geometrical parameter that can be determined on a lattice of resistors. It is a measure of the surface and volume currents and can hence be of value in the study of shaly rock, where the surface conduction may be large. In permeability problems it is rigorously related to the high-frequency, ac permeability, where the flow is a potential flow problem like the conductivity. At low frequencies and dc, $\Lambda$ is not rigorously related to permeability, but it has properties that should make it a substantially better indicator than the volume-to-surface ratio alone. Because it is weighted by the electric field across the pore, it weights the pore-size distribution to reject dead-end pores and positively weights the pores carrying the largest currents. Banavar & Johnson (1987) have shown that $l_c$ and $\Lambda$ are related to each other within the approximations used to relate permeability to $l_c$. For systems modeled well by those approximations, $\Lambda$ may then be determined from mercury injection. Banavar et al (1988) have proposed that a novel dynamic measurement, in which the decay of a heat pulse is measured, can be used to estimate $\Lambda$. If connections to other physical properties can be made, then $\Lambda$ may become a valuable parameter connecting electrical, thermal, and flow properties that would facilitate remote measurements of permeability.

Doussal (1989) has considered several models that vary the shape and distribution of pores on the lattice. He finds cases where $l_c$ and $\Lambda$ are not equal and hence identifies several models that are not appropriate for rocks. In a tube model the permeability sensitively depends on the cross-sectional shape of the pores (Scheidegger 1960, Dullien 1979), and thus the constant in Equation (1) can take on essentially any value. But E. J.

Garboczi (submitted for publication) shows that for elliptical pores, the effective pore size determined from mercury injection is the one needed to define the hydraulic conductivity so that Equation (1) is independent of pore cross-section aspect ratio. In unpublished work we have also confirmed this result for triangular pore cross sections.

FRACTALS IN MERCURY INJECTION The patterns formed when fluids enter porous media have been studied in substantial depth. Lenormand (1989) summarizes three types of displacement: capillary fingering of one fluid into another when capillary forces dominate, viscous fingering when a less viscous fluid displaces a more viscous fluid, and stable displacement of a less viscous fluid by a more viscous one. Of the extensive literature on this subject, only the case where mercury enters an evacuated pore space is discussed here.

The earlier section on permeability pointed to work connecting the mercury-injection threshold to absolute permeability. This connection was based on percolation theory, which requires that the invading mercury form a percolation cluster on the pore-space network. Such a percolation cluster will be a fractal with $D_F = 2.5$ (Alexander & Orbach 1982). One consequence of the fractal mercury geometry is that the electrical conductivity as a function of mercury saturation is predictable from simulations on a network or by computing the probability that increases in saturation will create new connected, conducting paths (Thompson et al 1987b, Katz et al 1988). The experimental result shown in Figure 8 and numerical simulations both show that the electrical resistance changes in stepwise fashion as the mercury completes new conduction pathways. The resistance step sequence forms a "devil's staircase" of steps—a power-law

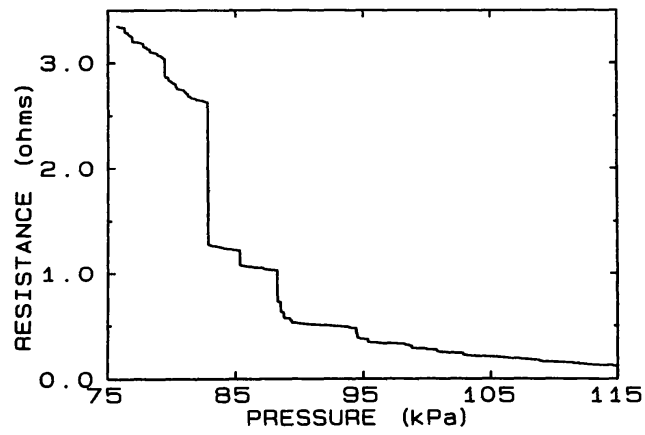


*Figure 8* The pressure dependence of the resistance for mercury injection into berea sandstone (Thompson et al 1987b).

distribution of steps, as shown in Figure 9, with an increasing number of steps detected as the resolution increases. Batrouni et al (1988) and Roux & Wilkinson (1988) also verify the power-law step distribution, while Katz et al (1988) show that the gravitational dependence of the step distribution is predictable from percolation theory in a potential gradient.

From visual inspection of injected Wood's metal patterns, Swanson (1979) called attention to the filamentary nature of partially saturated rock. Recently Clement et al (1987) measured directly the geometrical properties of Wood's metal injected into crushed glass. Correlation measurements showed that the Wood's metal formed a fractal structure with $D_F = 2.5$ between the grain size and 20 grain sizes. It is then well established from direct and indirect measures of geometry that the percolation model of mercury injection is appropriate, and hence that the assumptions behind Equation (1) are appropriate for rocks.

## RECENT ADVANCES

Work to date has shown that fractal pore structures are ubiquitous in sedimentary rock, that the correlations between pores are sufficiently random to apply percolation concepts to the study of flow through the pores, and that the old technique of measuring pore sizes with mercury injection actually gives information about the percolation structure (a fractal) formed by flowing fluids. Recent work suggests that capillary pressure also may be of use in measuring fractal properties of pore surfaces.

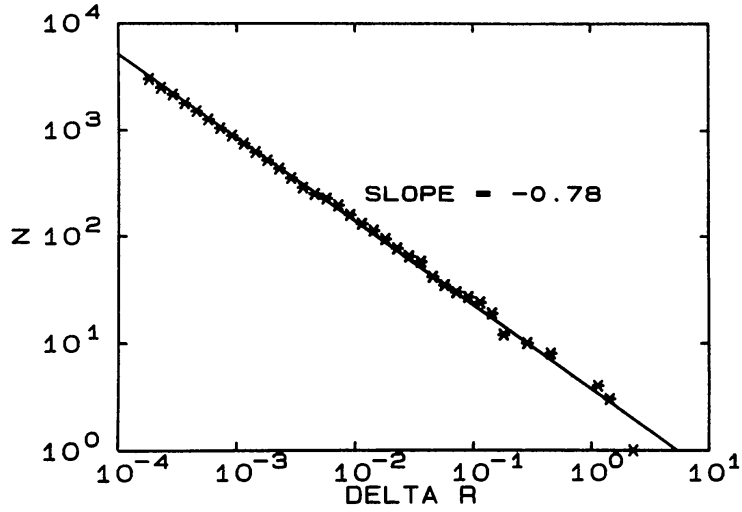


*Figure 9* The log-log plot of the number $N$ of resistance steps of size $\Delta R$ vs the resistance step size $\Delta R$ for the injection curve of Figure 8. The power-law relation indicates a "devil's staircase" of resistance steps, in agreement with a percolation model and simulation of injection into a finite sample (Thompson et al 1987b).

De Gennes (1985) pointed out that the capillary pressure curve for a porous medium with a fractal pore surface will have a power-law form at low wetting-phase saturation. This power-law form will occur when all of the fractal surface is fully connected to the pore body, so that accessibility to structure is not limited by penetration through smaller structure. For mercury injection this means that the high-pressure part of the injection curve will have a power-law form if all surface structure is equally accessible. Friesen & Mikula (1987) have applied these ideas to mercury injection in coal, where they find fractal structures in a few cases with $2.6 \leq D_F \leq 3$. Davis (1989) also has made the connection between water/air capillary pressure and fractal pore structure. Using published data, he finds that $D_F = 2.55$ for berea sandstone. Building on these suggestions, we have found that the high-pressure region of the injection curve for berea sandstone is a power law with an implied surface fractal dimension of 2.56, in agreement with Davis' calculation, and that $l_1 = 14$ nm and $l_2 = 1$ $\mu$m for this surface fractal (A. H. Thompson, to be published). The pore-volume fractal dimension for berea sandstone was previously measured to be 2.85 (Krohn & Thompson 1986). Additional data will be required to unambiguously connect capillary pressure to fractal structure, but if successful, this technique could become the fastest way to measure surface geometrical properties of porous media for a wide range of applications.

## ACKNOWLEDGMENTS

I thank my colleagues A. J. Katz, C. E. Krohn, and R. A. Raschke for their many contributions, and Po-zen Wong for the use of neutron-scattering data.

*Literature Cited*

Adler, P. M. 1989. Flow in porous media. In *The Fractal Approach to Heterogeneous Chemistry*, ed. D. Avnir, pp. 341–59. New York: Wiley

Aharony, A., Feder, J., eds. 1989. *Fractals in Physics*. Amsterdam: North-Holland. 283 pp.

Albano, E. V., Martin, H. O. 1989. Adsorption isotherms on fractal substrata. *Phys. Rev. A* 39: 6003–9

Alexander, S., Orbach, R. 1982. Density of states on fractals: "fractons." *J. Phys. (Paris) Lett.* 43: L625–31

Ambegaokar, V., Halpern, N. I., Langer, J. S. 1971. Hopping conductivity in disordered systems. *Phys. Rev. B* 4: 2612–20

Avnir, D., Farin, D., Pfeifer, P. 1983. Chemistry in noninteger dimensions between two and three. II. Fractal surfaces of adsorbents. *J. Chem. Phys.* 79: 3566–71

Avnir, D., Farin, D., Pfeifer, P. 1984. Molecular fractal surfaces. *Nature* 308: 261–63

Avnir, D., ed. 1989. *The Fractal Approach to Heterogeneous Chemistry*. New York: Wiley. 441 pp.

Bale, H. D., Schmidt, P. W. 1984. Small-angle X-ray-scattering investigation of submicroscopic porosity with fractal properties. *Phys. Rev. Lett.* 53: 596–99

Banavar, J. R., Johnson, D. L. 1987. Characteristic pore sizes and transport in porous media. *Phys. Rev. B* 35: 7283–86

Banavar, J. R., Johnson, D. L., Nagel, S. R. 1988. Thermal-wave spectroscopy: a new probe of porous media. *Phys. Rev. Lett.* 61: 2748–51

Batrouni, G. G., Kahng, B., Redner, S. 1988. Conductance and resistance jumps in finite-size random resistor networks. *J. Phys. A* 21: L23–29

Baudet, C., Bouchaud, J. P., Charlaix, E., Guyon, E., Hulin, J. P., et al. 1987. Transport in heterogeneous porous media. *Phys. Scr.* T19: 424–30

Berryman, J. G., Blair, S. C. 1987. Kozeny-Carman relations and image processing methods for estimating Darcy's constant. *J. Appl. Phys.* 62: 2221–28

Berryman, J. G., Milton, G. W. 1985. Normalization constraint for variational bounds on fluid permeability. *J. Chem. Phys.* 83: 754–60

Berryman, J. G., Milton, G. W. 1988. Microgeometry of random composites and porous media. *J. Phys. D* 21: 87–94

Bridge, J. S., Jarvis, J. 1982. The dynamics of a river bend: a study in flow and sedimentary processes. *Sedimentology* 29: 499–541

Brown, S. R. 1987. A note on the description of surface roughness using fractal dimension. *Geophys. Res. Lett.* 14: 1095–98

Brown, S. R., Scholz, C. H. 1985. Broad bandwidth study of the topography of natural rock surfaces. *J. Geophys. Res.* 90: 12,575–82

Charlaix, E., Guyon, E., Roux, S. 1986. Critical effects in the permeability of heterogeneous media. In *Fragmentation, Form and Flow in Fractured Media. Ann. Isr. Phys. Soc.* 8: 316–24

Clark, N. N. 1986. Three techniques for implementing fractal analysis of particle shape. *Powder Technol.* 46: 45–52

Clement, E., Baudet, C., Guyon, E., Hulin, J. P. 1987. Invasion front structure in a 3-D model porous medium under hydrostatic pressure gradient. *J. Phys. D* 20: 608–15

Davis, H. T. 1989. On the fractal character of the porosity of natural sandstone. *Europhys. Lett.* 8: 629–32

de Gennes, P. G. 1985. Partial filling of a fractal structure by a wetting fluid. In *Physics of Disordered Materials*, ed. D. Adler, H. Fritsche, S. R. Ovshinsky, pp. 227–41. New York: Plenum

Doussal, P. L. 1989. Permeability versus conductivity for porous media with a wide distribution of pore sizes. *Phys. Rev. B* 39: 4816–19

Drake, J. M., Klafter, J. 1990. Dynamics of confined molecular systems. *Phys. Today* 43(5): 46–55

Dullien, F. A. L. 1979. *Porous Media, Fluid Transport and Pore Structure*. New York: Academic

Farin, D., Peleg, S., Yavin, D., Avnir, D. 1985. Applications and limitations of boundary-line fractal analysis of irregular surfaces: proteins, aggregates, and porous materials. *Langmuir* 1: 399–40

Fleischmann, M., Tildesley, D. J., Ball, R. C. 1989. *Fractals in the Natural Sciences*. Princeton, NJ: Princeton Univ. Press. 200 pp.

Freltoft, T., Kjems, J. K., Sinha, S. K. 1986. Power law correlations and finite size effects in silica particle aggregates studied by small-angle neutron scattering. *Phys. Rev. B* 33: 269–75

Friesen, W. I., Mikula, R. J. 1987. Fractal dimensions of coal particles. *J. Colloid Interface Sci.* 120: 263–71

Fripiat, J. J., Gatineau, L., Van Damme, H. 1986. Multilayer physical adsorption on fractal surfaces. *Langmuir* 2: 562–67

Gueguen, Y., Dienes, J. 1989. Transport properties of rocks from statistics and percolation. *Math. Geol.* 21: 1–13

Hall, P. J. 1986. The fractal properties of microporous solids as determined by X-ray diffraction and adsorption techniques. *Chem. Phys. Lett.* 124: 467–69

Hansen, J. P., Skjeltorp, A. T. 1988. Fractal pore space and rock permeability implications. *Phys. Rev. B* 38: 2635–38

Hewett, T. A. 1986. *Fractal distributions of reservoir heterogeneity and their influence on fluid transport*. Presented at Annu. Tech. Conf. Soc. Pet. Eng., 61st, New Orleans (Pap. No. 15386)

Hough, S. E. 1989. On the use of spectral methods for the determination of fractal dimension. *Geophys. Res. Lett.* 16: 673–76

Huang, J., Turcotte, D. L. 1989. Fractal mapping of digitized images: application to the topography of Arizona and comparisons with synthetic images. *J. Geophys. Res.* 94: 7491–95. Also see: Goff, J. A. 1990. Comment on fractal mapping of digitized images: application to the topography of Arizona and comparisons with synthetic images. *J. Geophys. Res.* 95: 5159; Huang, J., Turcotte, D. L. 1990. Reply. *J. Geophys. Res.* 95: 5161

Hurd, A. J. 1988. Resource letter FR-1: fractals. *Am. J. Phys.* 56: 969–75

Hurd, A. J., Schaefer, D. W., Smith, S. M., Ross, S. B., Mehaute, A. L., et al. 1989. Surface areas of fractally rough particles studied by scattering. *Phys. Rev. B* 39: 9742–45

Johnson, D. L., Koplik, J., Schwartz, L. M. 1986. New pore-size parameter characterizing transport in porous media. *Phys. Rev. Lett.* 57: 2564–67

Kamath, J. 1988. *Evaluation of accuracy of estimating air permeability from mercury injection data*. Presented at Annu. Tech.

Conf. Soc. Pet. Eng., 63rd, Houston (Pap. No. 18181)
Katz, A. J., Thompson, A. H. 1985. Fractal sandstone pores: implications for conductivity and pore formation. *Phys. Rev. Lett.* 54: 1325–28
Katz, A. J., Thompson, A. H. 1986a. Comment on fractal sandstone pores. *Phys. Rev. Lett.* 56: 2112
Katz, A. J., Thompson, A. H. 1986b. Quantitative prediction of permeability in porous rock. *Phys. Rev. B* 34: 8179–81
Katz, A. J., Thompson, A. H., Raschke, R. A. 1988. Numerical simulation of resistance steps for mercury injection under the influence of gravity. *Phys. Rev. A* 38: 4901–4
Kay, B. H. 1986. The description of two-dimensional rugged boundaries in fine particle science by means of fractal dimensions. *Powder Technol.* 46: 245–54
Kirkpatrick, S. 1979. The geometry of the percolation threshold. In *Ill-Condensed Matter*, ed. R. Balian, R. Maynard, G. Toulouse, pp. 99–116. Amsterdam: North-Holland
Kopelman, R. 1988. Fractal reaction kinetics. *Science* 241: 1620–26
Krohn, C. E. 1988a. Sandstone fractal and Euclidean pore volume distributions. *J. Geophys. Res.* 93: 3286–96
Krohn, C. E. 1988b. Fractal measurements of sandstones, shales and carbonates. *J. Geophys. Res.* 93: 3297–3305
Krohn, C. E., Thompson, A. H. 1986. Fractal sandstone pores: automated measurements using scanning-electron-microscope images. *Phys. Rev. B* 33: 6366–74
Lenormand, R. 1989. Flow through porous media: limits of fractal patterns. *Proc. R. Soc. London Ser. A* 423: 159–68
Loehle, C. 1983. The fractal dimension and ecology. *Specul. Sci. Technol.* 6: 131–42
Lucido, G., Triolo, R., Caponetti, E. 1988. Fractal approach in petrology: small-angle neutron scattering experiments with volcanic rocks. *Phys. Rev. B* 38: 9031–34
Lukasiewicz, S. J., Reed, J. S. 1988. Specific permeability of porous compacts as described by a capillary model. *J. Am. Chem. Soc.* 71: 1008–14
Mandelbrot, B. B. 1982. *The Fractal Geometry of Nature*. San Francisco: Freeman. 461 pp.
Mandelbrot, B. B. 1986. Self-affine fractal sets. In *Fractals in Physics*, ed. L. Pietronero, E. Tosatti, pp. 3–28. Amsterdam: Elsevier
Mandelbrot, B. B., Wallis, J. R. 1968. Noah, Joseph and operational hydrology. *Water Resour. Res.* 4: 909–18
Meyer, Y. M., Farin, D., Avnir, D. 1986. Cross-sectional areas of alkanoic acids. A comparative study applying fractal theory of adsorption and considerations of molecular shape. *J. Am. Chem. Soc.* 108: 7897–7906
Nelkin, M. 1989. What do we know about self-similarity in fluid turbulence? *J. Stat. Phys.* 54: 1–15
Nigmatullin, R. R. 1989. The generalized fractals and statistical properties of the pore space of sedimentary rocks. *Phys. Status Solidi B* 153: 45–57
Nyame, B. K., Illston, J. M. 1980. Capillary pore structure and permeability of hardened cement paste. *Int. Symp. Chem. Cement Paste, 7th, Paris*, 3: VI 181–86
Orbach, R. 1989. Fractal phenomena in disordered systems. *Annu. Rev. Mater. Sci.* 19: 497–525
Orford, J. D., Whalley, W. B. 1983. The use of the fractal dimension to quantify the morphology of irregular-shaped particles. *Sedimentology* 30: 655–68
Pfeifer, P. 1987. Characterization of surface irregularity. In *Preparative Chemistry Using Supported Reagents*, pp. 13–33. London: Academic
Pfeifer, P., Avnir, D. 1983. Chemistry in non-integer dimensions between two and three. I. Fractal theory of heterogeneous surfaces. *J. Chem. Phys.* 79: 3558–65
Pfeifer, P., Wu, Y. J., Cole, M. W., Krim, J. 1989. Multilayer adsorption on a fractally rough surface. *Phys. Rev. Lett.* 62: 1997–2000
Power, W. L., Tullis, T. E. 1988. Relationship between spectral and divider methods for description of the fractal character of rock surface roughness. *Geol. Soc. Am. Abstr. With Programs* 20: A403 (Abstr.)
Roberts, J. N. 1986. Comment about fractal sandstone pores. *Phys. Rev. Lett.* 56: 2111
Rojanski, D., Huppert, D., Bale, H. D., Dacai, X., Schmidt, P. W., et al. 1986. Integrated fractal analysis of silica: adsorption, electronic energy transfer, and small-angle X-ray scattering. *Phys. Rev. Lett.* 56: 2505–8
Roux, J.-N., Wilkinson, D. 1988. Resistance jumps in mercury injection in porous media. *Phys. Rev. A* 37: 3921–26
Rubinstein, J., Torquato, S. 1989. Flow in random porous media: mathematical formulation, variational principles, and rigorous bounds. *J. Fluid Mech.* 206: 25–46
Scheidegger, A. E. 1960. *The Physics of Flow Through Porous Media*. Toronto: Univ. Toronto Press
Scholz, C. H., Mandelbrot, B. B., eds. 1989. *Pure and Applied Geophysics*, Vol. 131. Basel: Birkhäuser Verlag. 313 pp.
Schwartz, L. M., Sen, P. N., Johnson, D. L. 1989. Influence of rough surfaces on

electrolytic conduction in porous media. *Phys. Rev. B* 40: 2450–58
Sen, P. N. 1989. Unified model of conductivity and membrane potential of porous media. *Phys. Rev. B* 39: 9508–17
Shante, V. K. S. 1977. Hopping conduction in quasi-one-dimensional disordered compounds. *Phys. Rev. B* 16: 2597–2612
Sinha, S. K. 1989. Scattering from fractal structures. See Aharony & Feder 1989, pp. 310–14
Sinha, S. K., Sirota, E. B., Garoff, S., Stanley, H. B. 1988. X-ray and neutron scattering from rough surfaces. *Phys. Rev. B* 38: 2297–2311
Stanley, H. E. 1984. Application of fractal concepts to polymer statistics and to anomalous transport in randomly porous media. *J. Stat. Phys.* 36: 843–60
Stauffer, D. 1985. *Introduction to Percolation Theory*. London: Taylor & Francis. 124 pp.
Swanson, B. F. 1979. Visualizing pores and nonwetting phase in porous rock. *J. Pet. Technol.* 31: 10–18
Swanson, B. F. 1981. A simple correlation between permeabilities and mercury capillary pressures. *J. Pet. Technol.* 33: 2498–2504
Thompson, A. H., Katz, A. J., Krohn, C. E. 1987a. The microgeometry and transport properties of sedimentary rock. *Adv. Phys.* 36: 625–94
Thompson, A. H., Katz, A. J., Raschke, R. A. 1987b. Mercury injection in porous media: a resistance devil's staircase with percolation geometry. *Phys. Rev. Lett.* 58: 29–32
Torquato, S. 1990. Relationship between permeability and diffusion-controlled trapping constant of porous media. *Phys. Rev. Lett.* 64: 2644–46
Torquato, S., Beasley, J. D. 1987. Bounds on the permeability of a random array of partially penetrable spheres. *Phys. Fluids* 30: 633–41
Torquato, S., Lu, B. 1990. Rigorous bounds on the fluid permeability: effect of polydispersivity in grain size. *Phys. Fluids A* 2: 487–90
Weissberg, H. L., Prager, S. 1970. Viscous flow through porous media. III. Upper bounds on the permeability for a simple random geometry. *Phys. Fluids* 13: 2958–65
West, B. J., Shlesinger, M. 1990. The noise in natural phenomena. *Am. Sci.* 78: 40–45
Wong, P.-z. 1987. Fractal surfaces in porous media. In *Physics and Chemistry of Porous Media. II. AIP Conf. Proc. 154*, ed. J. R. Banavar, J. Koplik, K. W. Winkler, pp. 304–18. New York: Am. Inst. Phys.
Wong, P.-z. 1988. The statistical physics of sedimentary rock. *Phys. Today* 41(12): 24–32
Wong, P.-z., Howard, J., Lin, J.-S. 1986. Surface roughening and the fractal nature of rocks. *Phys. Rev. Lett.* 57: 637–40
Zick, A. A., Homsy, G. M. 1982. Stokes flow through periodic arrays of spheres. *J. Fluid Mech.* 115: 13–26